RIGOROUS PANORAMIC CAMERA MODEL FOR DISP IMAGERY

Toni SCHENK[1], Beatá CSATHÓ[2], Sung Woong SHIN[2]

[1]CEEGS Department
[2]Byrd Polar Research Center
The Ohio State University
Columbus, OH 43210, U.S.A
schenk.2@osu.edu; csatho.1@osu.edu; shin.111@osu.edu

KEY WORDS: Satellite Imagery, DISP Images, Corona Reconnaissance System, Panoramic Camera.

ABSTRACT

In the mid 90's, the U.S. government released images acquired by the first generation of photo reconnaissance satellite missions between 1960 and 1972. The Declassified Intelligent Satellite Photographs (DISP) from the Corona mission are of high quality with an astounding ground resolution of about 2 m. The KH-4A panoramic camera system employed a scan angle of 70^o that produces film strips with a dimension of 55 mm x 757 mm. Since GPS/INS did not exist at the time of data acquisition, the exterior orientation must be established in the traditional way by using control information and the interior orientation of the camera. Detailed information about the camera is not available, however. For reconstructing points in object space from DISP imagery to an accuracy that is comparable to high resolution (a few meters), a precise camera model is essential.

This paper is concerned with the derivation of a rigorous mathematical model for the KH-4A/B panoramic camera. The proposed model is compared with generic sensor models, such as affine, direct linear transformation, and rational functions. The paper concludes with experimental results concerning the precision of reconstructed points in object space.

The rigorous mathematical panoramic camera model for the KH-4A camera system is based on extended collinearity equations assuming that the satellite trajectory during one scan is smooth and the attitude remains unchanged. As a result, the collinearity equations express the perspective center as a function of the scan time. With the known satellite velocity this will translate into a shift along-track. Therefore, the exterior orientation contains seven parameters to be estimated. The reconstruction of object points can now be performed with the exterior orientation parameters, either by intersecting bundle rays with a known surface or by using the stereoscopic KH-4A arrangement with fore and aft cameras mounted an angle of 30o.

1 INTRODUCTION

During the past few years, several high-resolution spaceborne imaging systems have been launched and others will likely follow. The goal of mapping from space has become a reality. This second workshop about high-resolution mapping from space is testimony to the remarkable development and provides an excellent snapshot about the current status.

High-resolution mapping from space is not exclusively related to recent technology, however. In fact, it goes back to the early 1960s when Corona, the first satellite imaging system, was developed and successfully used in a highly classified program. The Corona camera delivered photography with a resolution of 2 m—a feat that only very recently has been surpassed. The veil on the super secret reconnaissance program was lifted in 1995 by an executive order. The declassified Corona imagery sets the clock of high-resolution mapping back to 1960. Almost one million images are now available to the public.

The Corona panoramic films, format $2.18'' \times 29.8''$ have a remarkable resolution of about 2 m. The polyester film base offers high stability. Thus, one can reasonably expect positional accuracies of features comparable to the resolution. This paper addresses the issue of determining positions in object space from measured points on Corona imagery as accurately as possible. The next section provides background information about the Corona program, including specifications about the camera and film. In Sec. 3 we describe the mathematical model for recovering the exterior orientation of the panoramic camera from control features in object space. This is necessary because the Corona missions were flown before the advent of GPS/INS. We also describe how to determine accurate positions of points in object space. We have performed several experiments with synthetic and real data to examine the feasibility of our proposed approach. Sec. 4 reports about some of the experiments. We conclude the paper with a brief summary about the major findings and point to future research related to the Corona imagery.

2 BACKGROUND

Two presidential orders had a great impact on reconnaissance from space. The approval of the Corona project by President Eisenhower in 1958 marked the beginning of the first satellite imaging reconnaissance system ever built. However, due to its highly secretive character, it benefited only a rather small group in the intelligence community.

The second presidential order related to Corona was issued 37 years later by President Clinton, requesting the declassification of the Corona imagery, including related documentation. This order benefits all those who are interested in using the high resolution imagery.

This section provides background information about the

Corona project, the cameras used, and the declassified images. For a more detailed account on Corona, the reader is referred to *McDonald* (1997).

2.1 Corona project

The Corona project started officially in February 1958 and continued until May 25, 1972, the day of the last mission launch. The project was jointly managed by the CIA and the US Air Force, involving a number of industrial partners, among them Lockheed as the prime contractor and responsible for the Agena spacecraft, and Fairchild and Itek that were resonsible for the Corona cameras.

The principle idea of Corona was to photograph targets of interest with a high resolution camera, and eject the exposed film in a capsule so that it can be retrieved after the mission. To achieve this goal, a reentry vehicle was designed that contained the thermally protected film capsule. The reentry vehicle was equipped with a retro-rocket, attitude control system, telemetry link, and parachutes. Mid-air recovery of the capsule was accomplished by C-130 airplanes that flew above the capsule, caught it with a line and hooks, and hauled it into the open cargo area. If mid-air recovery failed, a back-up water recovery with helicopter and ship would secure the capsule.

The capsule recovery system became a major challenge. It was not before the ninth mission that the first capsule with a film was successfully recovered (August 1960). From this moment, the reliability of Corona greatly improved. Out of 121 missions, 95 were successful. From 1963 to 1972, 69 missions were launched and only four ended unsuccessfully.

2.2 Corona cameras

Corona's reconnaissance cameras are referred to by the designator "KH" (from **K**ey**H**ole). Fairchild manufactured the first two cameras, KH-1 and KH-2, that were flown on five successful missions from 1960 to 1961. Other Corona cameras included KH-3 (operated from 1961-1962), KH-4 (1962-1963), KH-4A (1963-1969), and KH-4B (1967-1972), all designed, revised and manufactured by Itek. On the majority of the 95 successful Corona missions, the KH-4, KH-4A and KH-4B cameras have been used. These three cameras are very similar and we summarize their most important properties.

The KH-4 is a twin panoramic camera with a convergence angle of 30^o. The lens system employs a Petzval configuration with five positive lenses and a focal length of $2'$. The lens barrel is about $3'$ and the distance from the first lens to the film is $4'$, resulting in a relatively bulky system. The lens constantly rotates about its rear nodal point and so does the slit that scans the image to the film. The film format is $2.18'' \times 29.8''$ and the scan angle is about 70^o. The film base is polyester and the film load capacity of KH-4A and KH-4B is $32,000'$, allowing a mission life of up to 19 days. In longer missions, the film would be ejected twice.

The f/3.5 aperture accommodates relatively slow film. Laboratory resolution tests rendered 280 lp/mm under high contrast conditions and 175 lp/mm for medium conditions. Under operational conditions, up to 160 lp/mm were reached. This translates to a ground resolution of 2 m ($6'$) for orbits as low as 80 nm. In order to achieve this resolution, image motion compensation (IMC) is essential. During the scan time, the platform moves and the Earth rotates. The Corona cameras compensated these anticipated movements by rotating the optics synchronous to the scan. The magnitude of the IMC was programmed and entered into the control unit prior to a mission.

Panoramic cameras are ideal for reconnaissance purposes. For one, the ground coverage is impressive. For example, the KH-4 camera scan angle of 70^o produces a swath width of approximately 231 km. Moreover, the resolution is uniform and there is no decrease of illumination toward the corners. These advantages come at the cost of a more complex imaging geometry. It stands to reason to expect a positional accuracy of measured features comparable to the resolution. That is, the position of well identified points should be 2 m in object space. With this goal in mind, Sec. 3 proposes a suitable mathematical model.

2.3 Declassified Imagery

The second presidential order related to Corona had and is continue to have a great impact on the mapping community. On February 22, 1995, President Clinton issued an executive order to declassify all the Corona satellite reconnaissance images, including related documentation and equipment, such as the Corona camera and the reentry vehicle that returned the film in a capsule. The **D**eclassified **I**ntelligence **S**atellite **P**hotographs are known as DISP images. The US Geological Survey (USGS) is charged with archiving and distributing the declassified imagery. The EROS Data Center in Sioux Falls stores and disseminates over 866,000 images.

Access to the DISP catalog is facilitated by browse images (JPEG) that can be viewed on-line before ordering the films. Information about the images, such as geographic area and date, is also accessible through Internet. Products are available at modest cost and include film positives or negatives ($18) and paper prints ($14).

3 MATHEMATICAL MODEL FOR KH-4A/B IMAGERY

in order to determine object space positions of features measured on Corona images, the exterior orientation must be known. For the panoramic stereo cameras KH-4A and KH-4B, the exterior orientation comprises the position of the perspective center and the attitude of the camera at any instance an image element is formed. We consider a slit as such an elementary image. Consequently, a Corona film strip has theoretically an infinite number of exterior orientation parameters.

During the Corona project, the exterior orientation was derived from orbit information and information obtained from

auxiliary cameras, such as stellar and horizon cameras. Since not all necessary information for a precise exterior orientation is readily available, we propose a solution that is independent from orbital and star tracker data. The solution is based on known information in object space, such as control points and control features.

3.1 Indirect exterior orientation with control features

The collinearity model establishes a convenient relationship between image and object space by enforcing the condition that the perspective center, a point in object space and its image are on a straight line. This simple condition holds as long as the camera (perspective center and image) and the object point remain constant during the time of exposure. In the case of a panoramic camera, this is only true for a fixed slit position. We derive in the following the collinearity model for the slit at time t and then generalize for the entire strip. With strip we refer to one scan sweep of the panoramic camera.

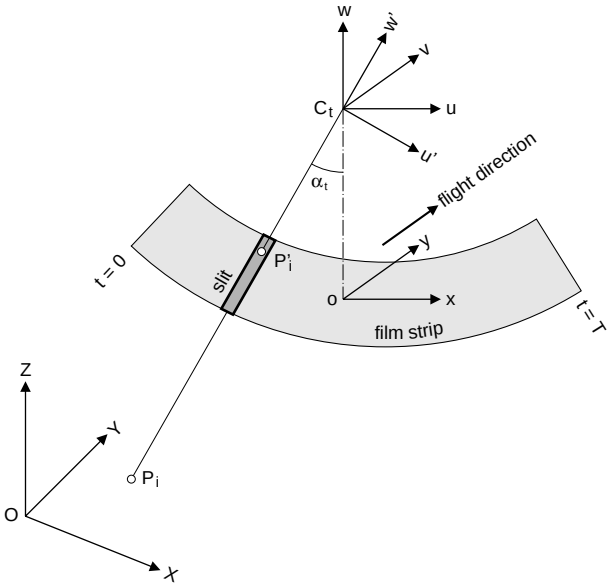

Figure 1: Illustration of object space and image space coordinate frames. The film is shown as a positive.

Let $O-XYZ$ be the object space coordinate frame, and let $C_t - uvw$ be the camera coordinate frame with the origin at the perspective center C_t at scan time t. As illustrated in Fig. 1, the $v-$axis is parallel to the flight direction and the $w-$axis is pointing near vertical. Next, let $C_t - u'v'w'$ be the slit coordinate system with the negative $w'-$axis pointing to the position of the slit, again at scan time t. The origin and the $v'-$axis are identical to the respective quantities of the camera frame. Now, let $o-xy$ denote the 2D image space coordinate frame with the origin, o, at the intersection of the $v-$axis with the positive film and with the $x-$ and $y-$axes parallel to the $u-$ and $v-$axes of the camera system, respectively. Then, the image coordinates (x_i, y_i) of a point P'_i are related to the camera coordinates by $[x_i\ y_i\ -f] = \lambda_i[u_i\ v_i\ w_i]$ with f the focal length and λ_i a scalar that differs from point to point.

The slit moves from one end of the cylindrical image plane to the other one during the scan time T. This movement can also be described by angle α as indicated in Fig. 1. Thus, α_t refers to the angle between the negative $w-$axis and slit position at scan time t. That is,

$$\alpha_t = x_i/f \tag{1}$$

with x_i the image coordinate of point P'_i.

Let $\mathbf{p}_i$ be the vector to object point P_i and $\mathbf{c}_t$ the vector to the perspective center at time t in the object space coordinate frame. The collinearity condition for points in slit t can now easily be expressed as

$$\mathbf{m}'_i = \mathbf{R}(t)(\mathbf{p}_i - \mathbf{c}_t) \tag{2}$$

with $\mathbf{m}'_i = [0\ v'_i\ w'_i] = 1/\lambda_i[0\ y_i\ -\mathrm{f}]$ the image vector in the slit system. $\mathbf{R}(t)$ is a 3D orthogonal rotation matrix that expresses the attitude (pitch, roll, azimuth) of the camera system with respect to the object space at scan time t. Let $\mathbf{m}_i$ be the image vector in the camera system. Then we have $\mathbf{m}_i = \mathbf{R}_\alpha \mathbf{m}'_i$, with $\mathbf{R}_\alpha$ a 3D orthogonal rotation matrix defined by a rotation of angle α_t about the $v-$axis as follows

$$\mathbf{R}_\alpha = \begin{bmatrix} \cos\alpha_t & 0 & \sin\alpha_t \\ 0 & 1 & 0 \\ -\sin\alpha_t & 0 & \cos\alpha_t \end{bmatrix} \tag{3}$$

The collinearity condition for one swath can now be expressed as $\mathbf{m}_i = \mathbf{R}_\alpha \mathbf{R}(t)(\mathbf{p}_i - \mathbf{c}_t)$, or

$$\begin{bmatrix} 0 \\ y_i \\ -f \end{bmatrix} = \frac{1}{\lambda_i}\mathbf{R}_\alpha \mathbf{R}(t) \begin{bmatrix} X_i - X(t) \\ Y_i - Y(t) \\ Z_i - Z(t) \end{bmatrix} \tag{4}$$

Examining Eq. 4 reveals that the position, $[X(t)\ Y(t)\ Z(t)]$, and the attitude, $\mathbf{R}(t)$, are functions of the scan parameter t. Theoretically, this leads to an infinite set of exterior orientation parameters for one film strip. To cope with this problem, we now introduce the following assumptions. During the short scan time we assume that the attitude of the stabilized satellite platform remains constant, that is, $\mathbf{R}(t) = \mathbf{R}$. For the same reason, the satellite trajectory is assumed to be smooth during the scan time. Let $\mathbf{d} = [0\ D\ 0]$ be the vector that describes the change of the trajectory in the flight direction during one scan, where $D = v \cdot T$ is the travel distance, v the velocity of the satellite, and T the total scan time of the panoramic camera. Then, any intermediate position is determined by multiplying $\mathbf{d}$ by a scalar, s that is proportional to t/T, or equivalently

$$s = x_i/L + 0.5 \tag{5}$$

with L the length of a Corona film strip (see also Fig. 1).

With all these assumptions, we can approximate the collinearity equations for one swath as follows:

$$\begin{bmatrix} 0 \\ y_i \\ -f \end{bmatrix} \approx \frac{1}{\lambda_i}\mathbf{R}_\alpha \left(\mathbf{R} \begin{bmatrix} X_i - X_o \\ Y_i - Y_o \\ Z_i - Z_o \end{bmatrix} - s \begin{bmatrix} 0 \\ D \\ 0 \end{bmatrix} \right) \quad (6)$$

As usual, scalar λ_i can be eliminated by dividing the first two component equations by the third one. This will leave us with two equations for every measured point P_i and a total of seven unknown parameters: $[X_o\ Y_o\ Z_o]$ are the coordinates of the perspective center at the beginning of one swath; pitch, roll, and azimuth are the three independent angles of the rotation matrix $\mathbf{R}$; and D is the total travel distance of the satellite during one scan sweep. All other quantities in 6 are known: $[X_i\ Y_i\ Z_i]$ are the control point coordinates in object space; $\mathbf{R}_\alpha$ is defined by Eqs.1 and 3; $[x_i\ y_i]$ are the measured control points, and f is the focal length.

Eq.6 serves as a starting point for determining the seven orientation parameters by an adjustment procedure, e.g. least-squares. Approximations are readily obtained from the trajectory information that comes along with DISP imagery. We skip the details of deriving the adjustment procedure and refer the interested reader to *Shin* (2003).

3.2 Space intersection

The KH-4 twin panoramic cameras provide stereo capabilities. The fore and aft cameras have a convergence angle of 30^o. With the exterior orientation known, we can compute 3D positions of points in object space provided they are measured on overlapping fore and aft images.

To obtain points, P_i, in object space we rearrange Eq. 6 as follows:

$$\begin{bmatrix} X_i \\ Y_i \\ Z_i \end{bmatrix} = \lambda_i \mathbf{R}\mathbf{R}_\alpha \begin{bmatrix} 0 \\ y_i \\ -f \end{bmatrix} + \mathbf{R}^T \begin{bmatrix} 0 \\ s \cdot D \\ 0 \end{bmatrix} + \begin{bmatrix} X_o \\ Y_o \\ Z_o \end{bmatrix} \quad (7)$$

The unknowns comprise the position $P_i = [X_i\ Y_i\ Z_i]$ and scalar λ_i. All the other quantities are either measured or known from the exterior orientation. Note that the x_i-coordinate does not appear explicitly. It is used in Eqs. 1,3, and 5, however. Measuring the same point P_i on the fore and aft images provides six equations with two scale parameters and three positions to be determined. Again, a least-squares adjustment solves this problem.

4 EXPERIMENTAL RESULTS

We have tested the proposed algorithms for determining the exterior orientation of Corona images and the space intersection with synthetic data and a variety of real data sets, (*Shin* (2003)). This section presents some of the results obtained with a fore and aft Corona KH-4A image stereo pair. Table 1 contains relevant mission data and other information. Film positives and meta-data of an area in mid-Ohio were obtained from USGS (see Sec. 2.3).

Table 1: Mission data of Corona KH-4A images used for experiments.

	fore image	**aft image**
identifier	DS1026-1014DF005	DS1026-1014DA011
time	October 29, 1965	October 29, 1965
# control pts	33	31
# check pts	33	33

We scanned the B/W film with a pixel size of 12 μm. Since the active scan area of photogrammetric scanners is limited to aerial film formats (9 in $\times$ 9 in), the DISP film had to be scanned in portions. Using identical features in the overlapping area, a similarity transformation established a common film frame. Fig. 2 depicts a small image patch, size 12 mm $\times$ 9 mm, demonstrating the high resolution of Corona images. The walkways in the oval are approximately 3 m wide.

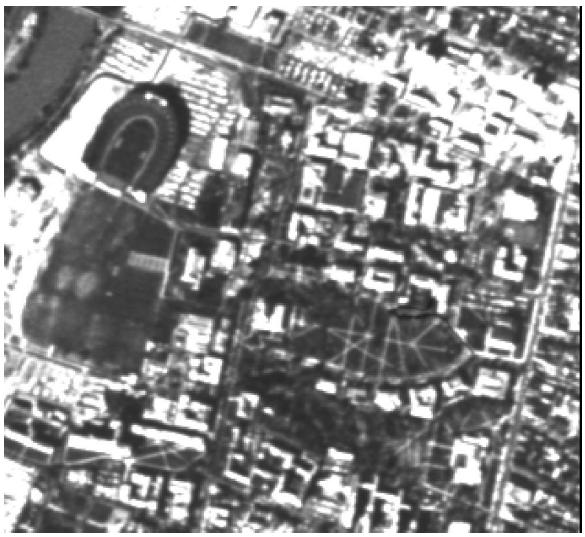

Figure 2: Small portion of a Corona image depicting a part of the OSU campus and the stadium, demonstrating the high resolution. For eample, the walkways in the oval are approximately 3 m wide and covered by 2 to 3 pixels.

4.1 Performance of proposed model

4.1.1 Exterior orientation The exterior orientation as described in Sec. 3.1 was performed with 33 control points in the fore and 31 control points in the aft image. The meta-data provided approximations for X_o, Y_o, Z_o. Initial values for the azimuth were estimated from a 2D similarity transformation with the measured control points and the position of the control points in object space.

We have identified suitable control and check points on DRGs (Digital Raster Graphs: digitized USGS quadrangle maps, scale 1:24,000, $7.5'$ quadrangle grid) by displaying them side by side with the digitized film. Considering the

time difference of 20 to 30 years between maps and satellite images, finding identical points was a challenge at times. We estimate the accuracy of identifying and measuring the points on the 1:24,000 maps to ± 5 m.

There is no independent check of the results of the exterior orientation. For assessing the accuracy we rely on the statistics from the adjustment procedure that should be quite reliable considering the large redundancy of $r = 33{\cdot}2{-}7 = 59$. The variance component for both images is 14 μm or 1.2 pixels. The standard deviations for X_o, Z_o is approximately half a meter. The Y_o coordinate has a higher value in both images (1.8 m and 1.3 m, respectively). The angular components have standard deviations well below $\pm 1''$ with the exception of the pitch that reaches $\pm 1.8''$ and $\pm\, 1.4''$. Considering the short width of the film compared to its length ($2.25'' \times 30''$) we are not surprised to see that Y_o and the pitch is less accurate than the other components.

4.1.2 Intersection of points in object space A more independent assessment of the overall accuracy is possible by using check points. We have selected 20 points in the center part of the overlapping fore and aft images and computed the $X-, Y-, Z-$coordinates with the proposed space intersection algorithm. The same points were measured on the digital maps. The table below contains the results of comparing the computed positions with the measured positions.

Table 2: Accuracy of computed positions of check points by space intersection.

RMS		
X [m]	Y [m]	Z [m]
6.15	5.62	12.34

The numbers listed in Table 2 are root mean square errors, RMS $= \sqrt{[d \cdot d]/n}$ with d the differences between computed and known positions, and n the number of points. In judging the results one should bear in mind that the check points have also errors, probably on the order of a few meters (according to National Map Accuracy Standards 7.44 m for location and 0.9 m for elevation). We conclude that the location accuracy corresponds to about one pixel ($12\,\mu$m $\times\, 3.05 \cdot 10^5$). The elevation accuracy is slightly larger than expected. The convergence angle between fore and aft camera of 30^o corresponds very nearly to a B/H (base height ratio) of a normal stereo model, which have a reasonable error propagation for elevations. However, the pitch error is considerably larger than the other angular errors. The pitch error directly affects elevations.

The intersection of points in object space depends on the exterior orientation. Thus, the results reported here also confirm the accuracies achieved with exterior orientation. In fact, the processes of indirect exterior orientation and object space reconstruction are closely intertwined and have the nice property that modeling errors, for example in the camera model, cancel out (*Schenk* (1999), p. 389-392).

4.2 Comparison with other approaches

We now compare the proposed approach with other image registration and reconstruction methods. Arguably, the most popular method to register images (image to image, image to map), is rubber sheeting. Here, a low order 2D polynomial is fitted through data points and control points in order to transform an image to another image or to a map. The polynomial coefficients are then used to transform non-control points. The simplest transformation in this scheme is an affine transformation. This approach cannot take topographic surfaces into account, nor can it cope with more complex camera models.

Recently, the **R**ational **F**unction **M**odel, RFM, has gained popularity. Its chief advantage is that higher order polynomials offer a way to circumvent an explicit modeling of the imaging sensors. This is of particular interest in situations where the camera model is unavailable. Several feasibility studies, e.g. *Tao et al.* (2000), *Dowman et al.* (2000), demonstrate the effectiveness of RFM.

We have used the fore and aft panoramic stereo pair to register both images to the same control points we have used for the exterior orientation (Sec. 3.1). Next, we transformed the check point coordinates with the registration parameters to the object space and compared their location with the corresponding points measured on the digital map. Since the 3D reconstruction from a 2D image has one degree of freedom, we used the elevations from the map.

Table 3: Accuracy comparison of proposed algorithm with other methods.

image	**affine**		**RFM**		**OSU**	
	σ_x	σ_y	σ_x	σ_y	σ_x	σ_y
fore	703.92	165.00	16.53	8.68	9.09	8.31
aft	1038.20	109.21	35.55	8.12	8.78	9.48

Table 3 contains the result of this comparison test, expressed as standard deviations obtained from the differences between computed and known location. As was to be expected, the affine model with errors on the order of hundreds of meters does not produce acceptable results at all. Unless applied to very small parts of the image where distortions resulting from the panoramic camera model and the topography are small, this simple form of rubber sheeting should not be used.

The 2^{nd} order RFM model fares much better but it is still inferior to our proposed approach. Not only are the errors larger but the outcome is less predictable and an optimal solution is often found experimentally.

The results of our approach, labeled "OSU" in Table 3 is consistent with those obtained from the stereo intersection.

5 CONCLUSIONS

The declassified intelligence satellite photographs (DISP) provide exciting opportunities. Earth science applications

in particular benefit from the high quality images. Research related to change detection, for example urban expansion, ice sheet dynamics, soil erosion use DISP images to establish a baseline in time series studies. For example we obtained baseline velocities of fast moving outlet glaciers in Greenland to investigate if on-going changes are significantly different from the long-term trend, see *Csathó et al.* (1999), *Thomas et al.* (2000) and *Csathó et al.* (2002).

The goal of this study was to develop suitable algorithms that would allow to determine positions of features in object space with an accuracy that is comparable with the high resolution of DISP imagery. In the case of Corona images the resolution is about 2 m. We have developed a two-step approach. First, the exterior orientation of the Corona camera is determined using known ground features, such as control points and control lines. The second step is concerned with intersecting features in object space from their measurements on stereo pairs. For this, the exterior orientation is a prerequisite.

We have demonstrated the feasibility of the proposed method with an example of a Corona stereo pair, covering an area of 13 km $\times$ 230 km in mid-Ohio. The film was digitized with a pixel size of 12 μm and the measuring accuracy is estimated to be one pixel. Multiplying the measuring accuracy with the scale (approx. 1:300,000) gives a crude but useful estimation of the accuracy of computed features in object space. The results obtained with 20 check points confirmed that this expected accuracy can be reached.

We also compared our approach with other methods, for example affine transformation, direct linear transformation, and rational function model. As one would expect, an affine transformation is totally inadequate to cope with the geometry of panoramic cameras. The rational function models performs well but it requires more control points.

We are currently performing more experiments with Corona panoramic imagery, including GPS check points, and matching stereo pairs for deriving DEMs automatically. We also fuse Corona imagery with other sensory data for the purpose of change detection.

References

Csathó, B. M., J. F. Bolzan, C. van der Veen, T. Schenk and D-C. Lee (1999). Surface velocities of a Greenland outlet glacier from high-resolution visible satellite imagery. *Polar Geography*, **23**, 71-82.

Csathó, B., T. Schenk, S. Shin and C. J. van der Veen (2002). Investigating long-term behavior of Greenland outlet glaciers using high resolution imagery. *Proceedings of IGARSS 2002*, published on CD-ROM.

Dowman, I., J. Dollof (2000). An evaluation of rational functions for photogrammetric restitution. *ISPRS Intern. Archives*, **33**(B3), 254–266.

McDonald, R. (1997). *Corona between the Sun and the Earth*. ASPRS, 5410 Grosvenor Lane, Bethesda, Md., 440 p.

Schenk, T. (1999). *Digital Photogrammetry*. TerraScience, Laurelville, OH 43135, 428 pages.

Shin, S. W. (2003). *Rigorous Model of Panoramic Cameras*. Diss., Dep. of Civil and Environmental Engineering and Geodetic Science, OSU, 81 p.

Tao, V., Y. Hu, B. Mercer, S. Schnick and Y. Zhang (2000). Image rectification using a generic sensor model-rational function model. *ISPRS Intern. Archives*, **33**(B3), 874–881.

Thomas, R. H., W. Abdalati, T. Akins, B. Csathó, E. Frederick, P. Gogineni, W. Krabill, S. Manizade and E. Rignot (2000). Substantial thinning of a major east Greenland outlet glacier. *Geophysical Research Letters*, **27**(9), 1291-1294.